Physics of complex metals: Temperature-dependent resistivities in ionic superconductors and stable quasicrystals

J. C. Phillips
AT&T Bell Laboratories, Murray Hill, New Jersey 07974
(Received 16 October 1991; revised manuscript received 26 May 1992)

Elementary phase-space arguments for electron-phonon scattering in metals give the temperature-dependent resistivity $\rho(T) \sim T^n$ with $n \geq 3$. Similarly for electron-electron scattering $n=2$. To explain $n=1$ for superconductive $(Bi,Sr)_4CuO_{6+\delta}$ over the range $7 < T < 700$ K one can assume a structural model with punctured semiconductive domain walls. There is strong evidence for this model not only in oxide perovskites, but also in Chevrel compounds such as $EuMo_6S_{8-y}O_x$, which also exhibit linear $\rho(T)$ over a narrower temperature range. In the domain-wall model recoil energy and momentum are absorbed by the walls, much as umklapp momentum is absorbed by the crystal as a whole in pure polyvalent metals. A wide range of experimental data support the model. By-products of the model are explanations of carrier freeze-out as measured by diverse anomalies in the Hall resistance, the correlation of T_c with the slope of the linear background tunneling conductance of Pb-Bi-O superconductors, a simple qualitative explanation for the first- (second-) order electronic (structural) phase transition observed near $x=0.21$ in well-annealed $La_{2-x}Sr_xCuO_4$, and an explicit mechanism for the origin of c-axis linear resistivities in intercalated Bi-Sr cuprates. A similar microstructural model explains the linear temperature dependence of the hopping conductance in stable ternary quasicrystals. The key factor common to both ionic superconductors and stable quasicrystals is their multinary composition which creates hierarchies of saddle points in the local conductance.

I. INTRODUCTION

In the past decade the two new kinds of materials with the most novel electronic properties have both been ternary (or multinary) systems. The first kind consists of the high-temperature superconductors and includes not only cuprates with pseudoperovskite structures but also the pseudoternary perovskite alloys $(Ba,K)(Pb,Sb,Bi)O_3$. These materials have attracted world-wide attention and their properties have been studied more extensively than those of any other kind of inorganic solids except semiconductors such as Si, Ge, and GaAs. While the relations between electronic properties (including doping) and structure in the latter were explained easily and successfully by theorists, this has not yet been the case for high-T_c superconductors. The second case consists of stable quasicrystals such as Al-Cu-Fe. Here again electronic anomalies have been discovered which are quite unexpected for alloys of three metallic elements.

It is the thesis of this paper that the origin of the novel electronic properties of these materials lies in their multinary structures, which create the possibility of extensive inhomogeneous micromorphologies which cannot be obtained with binary materials such as Nb_3Sn or NbN superconductors (in the first case), or Pd-Si metallic glasses (in the second case). This paper explains these inhomogeneous micromorphologies in detail, but the evidence for the models is largely circumstantial. The nature of the models itself shows that this is unavoidable, but the reader should realize that the models are inherently plausible. The reason is that there are substantial phenomenological differences between the structural systematics of binaries and ternaries which have emerged from extensive statistical studies of Villars and co-workers. A recent paper[1] discusses these results and connects them to the properties of superconductivity, quasicrystallinity, and ferroelectricity. The essential point is that ternary or multinary compounds are inherently more complex than binary compounds, with the ternary ABC structure being formed from AB and AC building blocks. These building blocks, and the defects associated with them, lead to a wide variety of possible micromorphologies, and a few of these are probably responsible for the above-mentioned novel electronic properties.

It is important to realize that, while complex structures may be necessary to produce electronic anomalies, they are not sufficient. The sufficient conditions are satisfied only to some extent by accident. This is an essential feature of the present models and what the accidental conditions are will become apparent as the models unfold. Experimentally these conditions are discovered essentially by trial and error. The theory developed here contains little mathematics and this also is a matter of design. I do not pretend to be able to determine from first principles the many delicate microscopic parameters which would be needed to explain quantitatively the electronic properties of complex metals. I will show, however, that many apparently unrelated electronic anomalies can be qualitatively understood by a single model based on spatial inhomogeneities. This theory is therefore designed to be different from conventional theories which introduce many adjustable parameters to explain with a simplistic conventional model a single experiment, and then use completely different sets of parameters to ex-

plain different experiments on the same or related alloys. Also, most conventional theories do not discuss chemical trends at all, but phase diagrams provide the best quantitative evidence for the main features of the present models.

The reader may wish, before proceeding further with this paper, to study the systematics of complex metals as described in Ref. 1. This paper exhibits many similarities between structural trends in complex metals and in high-temperature ferroelectrics[2] such as $La_2Ti_2O_7$ and $Bi_4Ti_3O_{12}$ ($T_c = 1770$ and 950 K, respectively). It is important to realize that these systematics arise from cluster structures which are absent from binary and elemental systems. It is also important to realize that these structural systematics may well explain, as the model here assumes, why compositional trends in electronic stabilization energies (as measured by transition temperatures) are generally so different in ternaries than in binaries.

The superconductive pseudoternary layered cuprates with high T_c's, such as $(La,Sr)_2CuO_4$ and $(YBa_2)Cu_3O_{7-x}$, exhibit many anomalous properties, but the one that has attracted the greatest theoretical interest so far is the linear temperature dependence of the (ab) planar resistivity with $d\rho/dT > 0$. This is evident over a very wide range of temperatures (7–700 K) in superconducting $Bi_{2+x}Sr_{2-y}CuO_{6+\delta}$ crystals,[3,4] while nonsuperconductive crystals exhibit semiconductive temperature dependences which have been fitted[5] by two-dimensional localization theory. Linear temperature dependence (over a necessarily narrower range of temperature) was observed previously[6,7] for $(La,Sr)CuO_4$ and $YBa_2Cu_3O_{7-x}$, and in specially prepared samples of the lower-T_c chalcogenide cluster Chevrel compound[8,9] "$PbMo_6S_8$." In all cases studied so far, both T_c and the linearity of $\rho(T)$ are quite sensitive to the method of sample preparation.

If we imagine that these materials are normal metals, then this temperature dependence is quite surprising. If the resistivity were due to electron-phonon scattering, it would vary[10] with a high power of T, $\rho(T) \sim T^n$ with $n \sim 3$. If it is due to electron-electron scattering, then Landau Fermi-liquid theory[11] gives $n = 2$. On the other hand, the resistivities in some of these materials are large ($\gtrsim 10^2$ Ω cm at room temperature), so we may suppose that we are near a metal-insulator transition, as in metallic glasses or ternary metastable quasicrystals.[12,13] However, there $n = 0$ with an $n = \frac{1}{2}$ correction term at low T and an $n = 1$ term at higher T, but with $d\rho/dT < 0$. In both cases the corrections are small [only of order 10^{-2} $\rho(O)$]. Thus, the linear anomaly with $d\rho/dT > 0$ is without precedent in either "good" or "bad" metals.

For these reasons I examine in this paper a structural model which is fundamentally different from those used to treat transport in simple homogeneous metals. The atomic structures of both the cuprates and the Chevrel compounds are characterized by a mixture of ionic and covalent (but not metallic) bonding, and this also applies to the family of pseudoternary perovskite superconductors $(K,Ba)(Pb,Bi)O_3$. (There are too few metallic electrons near E_F to affect the structure significantly.) The dominant scattering mechanism is not electron-phonon or electron-electron, but electron-defect. In metals, electron-defect scattering makes the resistivity constant ($n = 0$, the "residual resistivity" of elemental or binary metals). This is easily explained by homogeneously distributed scattering by point defects. So long as the electron mean free path l is much larger than the average spacing s of these defects, the metal can be treated within the random-phase approximation as homogeneous with a constant, temperature-independent scattering rate.

Our pseudoternary materials, however, have different kinds of chemical bonding and there is no reason to suppose that all the defects are point defects. In transition-metal oxides planar defects have been identified by electron microscopy.[14] The resistivity ρ of NbO_x (which is not superconductive) is linear[14] over a very wide temperature range (77–900 K) for x in the last 3% of the upper end of the homogeneity range measured by diffraction, with ρ fully metallic (similar to Nb). In the cuprates there is a wide variety of evidence that indicates the presence of insulating or semiconductive domain walls (which may or may not be twin boundaries). The evidence comes from the oxygen isotope effect (where the oxygen in the domain walls is not exchanged, although that in the domains is fully exchanged[15]) and from Ni and Zn substitution for Cu in the CuO_2 planes of $YBa_2Cu_3O_{7-x}$ (where Zn precipitates in the domain walls but Ni does not[16]). As we will see in this paper, such domain walls, forming insulating or nearly insulating networks, are needed to resolve other anomalies in NbO_x, the ionic-covalent Chevrel compounds and perovskites.

On the one hand, it may seem that this structural model represents only a small extension of what is already known. Certainly the factor limiting T_c in all high-temperature metallic superconductors is lattice instabilities,[17] and the present model merely extends this idea to the regime of domain walls which are characteristic of ionic-covalent bonding, for instance, in ternary ferroelectrics.[1] Yet all the theories of electrical resistivity mentioned above assume micromorphological homogeneity on an atomic scale, presumably because it seems that there are too many kinds of larger-scale microscopic inhomogeneities; as we shall see, this is actually not the case. At the same time, the present theory is completely different from available alternative theories of the linearity of $\rho(T)$, which are entirely electronic in nature and which have assumed that high-T_c superconductivity is caused not by electron-phonon interactions but by some kind of electron-electron interaction. Careful examination of these theories shows, as we shall see in Sec. VI, that they do not explain high-T_c superconductivity nor the correlation of $\rho(T)$ linearity with T_c. In fact, they do not even explain chemical trends in $\rho(T)$ itself. This leaves the present model as the only consistent description of the $\rho(T)$ linearity anomaly and its relation to high-T_c superconductivity.

Some general remarks concerning the structural differences between binaries and ternaries are in Sec. II. The connection to transport in the presence of spatial inhomogeneities is made in Sec. III, followed by a discussion of Chevrel compounds in Sec. IV, the

(K,Ba)(Pb,Bi)O_3 perovskites in Sec. V, the cuprates in Sec. VI, and a few comments on alternative homogeneous electronic theories are made in Sec. VII. The general view here is that the relation between structure and properties is so close that the two can be connected through a wide variety of indirect evidence. This approach has been successful for many complex materials, and it has previously been discussed at length.[17] The present paper extends that discussion with many examples based either on new data or new ideas needed to connect and explain older data. In Sec. VIII, I discuss Hall-effect anomalies, which appear to be consistent with my domain-wall model. In Sec. IX, I explain the origin of the correlation of T_c with the slope of the linear background tunneling conductance in perovskite superconductors. In Sec. X, I reconcile the first-order change in electronic properties with the continuous structural change which occurs in well-annealed $La_{2-x}Sr_xCuO_4$ at the orthorhombic-tetragonal transition at $x=0.21$. In Sec. XI, I explain the origin of the c-axis linear resistivity observed after intercalation in Bi-Sr cuprates. Finally, in Sec. XII, I discuss evidence for Fermi-level pinning defects in a very simple system, Cu-Zn (brass) alloys.

II. STRUCTURAL COMPLEXITIES AND REGULARITIES IN BINARY AND TERNARY COMPOUNDS

Quite a lot is known about the idealized crystal structures of high-T_c superconductors from diffraction data. This paper makes more explicit the suggestion made in many of my earlier papers on these materials[18,19] that high-T_c superconductivity is the result of an enhancement of $N(E_F)$ in some spatially connected regions by atomic defects in these structures. This suggestion has surprised many scientists because they suppose that such defects are always extrinsic with concentrations and spatial distributions which are not reproducible. By and large this view is correct for elemental and binary materials but it need not be correct for ternary and superternary (multinary) crystals. In this section I will explain why this qualitative change in structure occurs from binary to ternary compounds and why extensive defect arrays can be described as native (either metastable or stable) features of multinary crystals.

First I should remark that Wadsley (planar) defects can be observed[14] easily in transition-metal oxides T-T'-O, and that they are associated with the high densities of both cation and oxygen vacancies characteristic of these materials. Here we already have the emergence of clustering effects which may form complexes which restrict crystalline periodicity. The latter, of course, is still present and is responsible for Bragg diffraction, but when these diffraction patterns are refined they often give large R values indicative of incompletely periodic clustering effects (domains). Large R values are also characteristic of high-T_c cuprates, and they have been explained as the results of domain (orthogonal-tetragonal) or charge-density-wave formation, etc. They key point is that such effects are always qualitatively present and they are not incidental. They are difficult to quantify by diffraction, but they are strongly associated with the superconductive transition, as has been demonstrated, for example, by ion channeling.[20] The channeling experiments reveal that the Debye-Waller factors associated with a small volume fraction of the sample vary rapidly as T passes through T_c. The volume fraction must be small because Debye-Waller factors measured by linear averaging through powder neutron diffraction on the same material (for example, $YBa_2Cu_3O_{6.9}$) show no anomaly as T passes through T_c. No homogeneous or effective medium model can explain this paradoxical behavior, but it appears as a natural element of the present micromorphological model.

The structures of binary and ternary compounds can be organized systematically in the context of quantum structure diagrams.[1] The coordinates in these diagrams are compositionally weighted sums or differences of optimized elemental chemical factors such as valence electron number, atomic size and electronegativity, and melting points. When the compound-forming ability for binaries and ternaries is plotted using these coordinates, there are striking differences between binaries and ternaries (see Figs. 5, 6, and 8 of Ref. 1). The meaning of these differences is that in a ternary such as ABC, the structure generally consists of AC and BC building blocks. For the cuprate superconductors it may seem that this conclusion is obvious, as the layered structures are obviously separated into metallic CuO_2 layers and semiconductive or ionic layers such as BaO. This is indeed obvious for the ideal crystal structure as measured by diffraction. However, the key point of the approach based on quantum structural diagrams is that it is extremely general because it describes structural trends followed by thousands of compounds, layered or not. Thus, it is reasonable to assume that defects in ternary structures follow rules similar to those obeyed by the structure themselves. Such defects can be called native defects, to indicate that their properties are reproducible. One possible property of a native defect is that it may produce an electronic energy level which pins the Fermi energy. Such levels are often postulated for metal-semiconductor interfaces (Schottky barriers), but the simplest example of such an effect is found in Cu-Zn Hume-Rothery brass alloys (XII).

Another way of looking at Fermi-level pinning native defects in ternaries is to ask why they are so much more likely to occur in ternaries than in binaries or elemental metals. One could say simply that ternaries are more complex and thus offer more possibilities, but experience with high-T_c superconductors, stable quasicrystals, and high-T_c ferroelectrics[1] suggests that this answer is inadequate. In the simpler systems electronic anomalies associated with peaks in $N(E)$ for E near E_F can be suppressed by atomic relaxation of the Jahn-Teller type, where local bonding-antibonding splittings occur. An example is a simple-cubic metal with an s^2p^3 configuration such as Bi, where the sixfold coordination shell splits into two threefold shells with three empty long bonds and three occupied short bonds. The situation in pseudoternary (K,Ba)(Pb,Sb,Bi)O_3 perovskites proves to be much more complex and is discussed in detail below. The way

in which the structure is stabilized and made insulating (for instance, $Ba_{1-x}K_xBiO_3$ with $x \leq 0.37$) involves extensive planar defects which are feasible in a system with two building blocks, BaO and BiO planes, and this would be much less likely to occur in a binary solid. In the language of theoretical physics, it is much easier to break translational symmetry with extensive defect arrays in multinary compounds than it is in binaries and elemental metals because one set of defect clusters can act to stabilize or mechanically pin another set.

III. MODEL OF SPATIAL INHOMOGENEITIES

At present, Fermi-liquid theory is fashionable among theorists, especially those interested in low-temperature properties of very pure metals. In Landau Fermi-liquid theory it is argued on phase-space grounds[11] that electron-electron scattering must give rise to scattering at a rate Γ with $\hbar\Gamma \sim kT)^2/E_F$, where E_F is a relevant bandwidth. In good metals at room temperature, however, the resulting scattering rate is too small[11] by a factor of 10^4. For "bad" metals, even at low temperatures, the situation is even worse, since their resistivities, even at low temperatures, are $10-10^8$ larger than those of good metals at room temperatures.

There is another serious objection to electron-electron scattering alone as a source of resistivity: in a plasma, because of momentum conservation, this scattering has no effect on the total current. In a crystal only the crystal momentum is conserved, while the recoil associated with umklapp or reciprocal-lattice momentum can be absorbed by the crystal as a whole. For p and d electrons this provides an adequate momentum sink, but it also warns us that the phase-space argument alone is inadequate. Electrical resistivity results from momentum dissipation, not energy dissipation, of accelerated carriers, and in a complex solid there is no simple relation between the two.

What about domain walls? As we will see by many examples in the following sections, semiconductive domain walls explain many anomalies in the normal-state transport properties of multinary superconductors. Here we start not from a structural model based on an electron gas in a perfect crystal but from a two-phase system in which conductive domains are embedded in a semiconductive matrix through which all currents must pass. Such a matrix, with a distribution of barrier energies and thermally activated conduction across the barriers, can easily be used to describe the semiconductive $\rho(T)$ measured in nonsuperconductive materials, and will fit the data over a small range[5] of conductivities just as well as variable range hopping.[5] Now the processing parameters are varied experimentally to reduce the average barrier height, and we must ask how this changes the domain-wall properties.

In the spirit of homogeneous models one would say that such changes in processing reduce the barrier height uniformly, but from a structural point of view this seems extremely unlikely. Domain walls are native defects, which are introduced during sample growth of a multinary material with a complex unit cell and rigid ionic-covalent, bond-length–angle requirements. The domain walls reduce internal stress associated with incompatible elements in a way analogous to misfit dislocations at a heteroepitaxial interface. A good example is provided by $YBa_2Cu_3O_{7-x}$, where the as-grown value of x may be $\gtrsim 0.8$ (semiconductive material). Oxidation of the sample increases the conductivity of the CuO_{1-x} chains and at the same time introduces internal stress since the natural lattice constant (sometimes called the prototypical lattice constant) of the chains no longer matches that of the more rigid CuO_2 planes. Although T_c increases as x decreases, the smallest value of x is about 0.1. When x is forced below this value, two bulk phases develop,[21] the new phase with the smaller x also having a lower T_c. Thus, the domain walls are formed to reduce internal stress, which is intrinsically inhomogeneous. This means that the morphology of native domain walls cannot be described correctly by homogeneous averaging. Because the mechanically strongest element in the cuprates is the CuO_2 planes (with nearly constant lattice spacing, regardless of the composition of the boundary semiconductive layers such as BaO), it is there that the domain walls relieve stress. Thus, the walls are part of planes (which may be bent) which are normal to the CuO_2 planes and, in the case of YBCO, normal to the b-axis chains as well, in other words, ac planes.

Before we discuss a detailed model of the atomic-electronic structure of domain walls in these materials, it is important to emphasize the modifications of standard transport theory for homogeneous materials that are necessary to treat severely inhomogeneous systems. In classical metallic transport theory, all electrons carrying current are treated ballistically, which corresponds in quantum theory to using (Bloch) basis states which are eigenfunctions of crystal momentum. If we use a different set of basis states, for instance, standing waves obtained from the real and imaginary parts of the Bloch states, and neglect the phase relations between these states, we will calculate the conductivity incorrectly, in other words the validity of the Boltzmann equation and the relaxation time approximation appears to depend on the basis states used. Of course, this situation is unsatisfactory, and this problem is usually resolved by assuming that the scattering (by phonons or by impurities) occurs randomly in space and time when we use as basis states crystal momentum eigenfunctions. (This is sometimes called the random-phase approximation.) With this assumption of randomness one can derive the usual formulas for the temperature-independent residual resistivity of metals which contain a high density of irregularly placed point defects, as mentioned in the Introduction.

The scattering in the situations we will discuss is very far from random. At first one might think that it would be adequate to describe scattering of electrons from domain walls as elastic, just as scattering of Bloch waves by a periodic crystal potential is elastic. We note, however, that there is a hidden component in the scattering of Bloch waves which is inelastic in both momentum and energy (though usually only the inelasticity of the momentum scattering is emphasized), and this is umklapp scattering, where the recoil is absorbed by the crys-

tal as a whole. Here we must similarly use as basis states the eigenfunctions of the system *including the domain walls.* If the domain walls were to form a continuous network surrounding the domains, then all the basis states would be standing waves and the conductivity would be zero. If the defects are randomly distributed, then Bloch states are the correct basis states. The situations we will be considering are ones in which most of the basis states are standing waves so that most of the scattering takes place from current-carrying states into non-current-carrying defect states pinned by the domain walls. That is why we say that the recoil energy and momentum are absorbed by the domain walls, in close analogy with umklapp scattering in conventional metals. The reader should be warned that this is a subtle idea; like the idea of umklapp scattering itself, it is not obvious. (Nowadays the correctness of umklapp scattering is no longer questioned, but the idea encountered considerable resistance, especially from those schooled in classical transport theory, when Bloch discussed it in 1928–1932.)

Some readers have found the foregoing explanation of momentum dissipation satisfactory but are still puzzled by the issue of energy dissipation as Joule heat. In homogeneous systems one can derive the temperature dependence of $\rho(T)$ from momentum and energy conservation, after allowance is made for conventional umklapp, but this is no longer correct for inhomogeneous systems which are vicinal to metal-insulator transitions. When a current-carrying electron is scattered into localized states, there is local Joule heating and an increase in the effective local temperature of the domain(s) where those states are localized. Of course, this process is going on continually and equally in all domains and, unless some kind of electrical breakdown occurs, there will be no significant effects associated with what is still essentially uniform local heating. This is a problem with which experimentalists are quite familiar, especially in transport measurements of very pure metals at ultralow temperatures. The standard procedure is to ascribe nonlinearities to local heating at contacts, and to eliminate this by reducing the applied voltage and measuring smaller currents. Here, because of spatial inhomogeneities, the entire sample becomes, in effect, a network of contact barriers. Direct experimental evidence for native perovskite contact barriers is discussed in detail in Sec. IX.

There is another way of looking at the difference between the present phase-space arguments for inhomogeneous systems and the usual phase-space treatment of homogeneous systems. The latter conserves energy and particle number and corresponds to Boltzmann's microcanonical ensemble. The same results can be derived more generally by what is nowadays sometimes called a replica method, but what Gibbs called the grand canonical ensemble, in which a very large number of weakly connected similar systems are prepared with fluctuating particle numbers and energies, which are conserved only on the average. The domains and spatial inhomogeneities we are discussing represent a rather charming physical approximation to the grand canonical ensemble. At any instant in time the energy and density of current-carrying particles fluctuates from one domain to the next, and they are equal only on the average.

Some readers may still wonder where their favorite microcanonical phase-space reasoning broke down. The answer is that, for homogeneous systems, there are no localized valence states and $N_l(E_F)$, the density at localized valence states at $E=E_F$, is zero. This is no longer the case for the present system. Arguments that $N_l(E_F)\gg N_e(E_F)$, where e labels extended or ballistic states, will be given later in this section, and the experimental evidence which supports this assumption is discussed is Sec. IX. With local heating of localized states, the assumption of instantaneous energy conservation at constant temperature fails, and we have instead the much less restrictive situation of energy conservation at constant temperature only on the time average over all spatial domains, but not continually in each domain separately. Another important distinction between the present inhomogeneous model and conventional homogeneous models is that the elementary excitations which determine thermal properties (such as the specific heat) are very similar in the two cases, but there are large differences in the transport properties. This situation also arises for uncompensated semiconductor impurity bands, where there is a metal-insulator phase transition in the electrical conductivity but not in the specific heat or magnetic susceptibility when the impurity concentration is varied.[22] The reason there for the discordant transport and thermal properties is that the applied field itself partially separates localized and extended states. The important point is that nonequilibrium transport processes are much more subtle than equilibrium thermal ones, especially in inhomogeneous systems.

We next discuss the electronic structure of the domain–domain-wall interface. We picture this interface as a Schottky barrier analogous to metal-semiconductor interfaces. When such interfaces and their neighborhoods are decorated by point defects, the partial density of states associated with the defects, $N_d(E)$, consists of a series of peaks or resonances corresponding to the broadened localized states associated with the defects. If one of these peaks is centered at or near $E=E_F$, and if the concentration of defects is large enough, then we say that E_F is pinned at the interface by these defects. (These conditions are often satisfied in conventional Schottky barriers, and they have been studied by photoemission from semiconductor surfaces covered by $\lesssim 1$ monolayer of metal adsorbate.[22]) This situation can be described by the model shown in Fig. 1 for the spatially inhomogeneous density of states $N(E,\mathbf{r})$ which includes a metallic band contribution $N_b(E,\mathbf{r})$ and a defect contribution $N_d(E,\mathbf{r})$.

The interface in question may be a twin interface or antiphase boundary associated with orthorhombic symmetry. Planar defects of this type can be observed by electron microscopy and they have been examined in detail[23] for $La_{2-x}Sr_xCuO_{4-\delta}$. These planar defects of the orthorhombic or tetragonal space group merely provide a framework for planar arrays of the point defects which actually provide the perturbation of the crystal potential which, in turn, produces the electronic states that pin E_F.

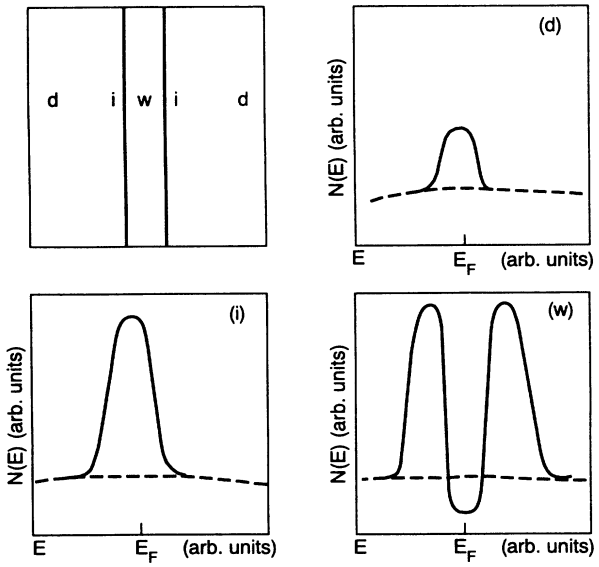

FIG. 1. The spatial variation of the peak in $N(\mathbf{r},E)$ associated with the defect states, $N_d(\mathbf{r},E)$, for E near E_F and for $\mathbf{r}$ in the domain (d), near the interface (i), and in the domain wall (w). The background density of band states, $N_b(E)$, is assumed to be slowly varying near E_F and is represented by dashed lines. The defect peak contributes to the total density of states $N(\mathbf{r},E)=N_b(\mathbf{r},E)+N_d(\mathbf{r},E)$ represented by the solid line. The function $N(\mathbf{r},E_F)$ reaches a peak for $\mathbf{r}=\mathbf{r}_i$ near the interface and drops (nearly) to zero inside a semiconductive domain wall (w).

These point defects may be oxygen vacancies or interstitials, for example, which are not observable directly by electron microscopy, but whose presence must be deduced by another kind of experiment, for instance, extended x-ray-absorption fine structure (EXAFS),[24] or combined x-ray- and neutron diffraction,[24] which lack spatial resolution. By comparing [001] and [011] ion channeling in $YBa_2Cu_{3-x}Fe_xO_7$, one can infer[25] that Fe dopants localize along [110], causing a change in twin orientations. Here the evidence for Fe localization near twins is quite direct, but one can reasonably infer that native point defects will be gettered by native planar defects. Electron microscopy has shown[25] the necessity for very large reconstructions of twin boundaries in YBCO for Ni and Zn doping, and quite different reconstructions for Fe and Al doping. This again emphasizes dopant segregation at or near planar defects.

From Fig. 1, we see that $N_d(E_F,\mathbf{r})$ is maximized at the domain–domain-wall interface where the point-defect concentration c is optimized at $c=c_i$. Well within the domain, $c<c_i$, while within the domain wall, $c\gg c_i$. It is clear that $N_d(E_F,c)$ will increase as c increases up to $c=c_i$. For $c>c_i$, inside the domain wall, defect pairing occurs and the defect resonance peak splits into two components, bonding and antibonding, separated by a pseudogap. Thus, although the integrated area under the peak is proportional to c, the value of $N(E_F,\mathbf{r})$ or $N(E_F,c)$ is maximized at $r=\mathbf{r}_i$ or $c=c_i$. Well inside the domain wall, $N(E_F)$ is small and the domain-wall center is either semiconductive or semimetallic. The wall thickness associated with pairs of microtwins or antiphase boundaries may be of order[23] 50 Å, while the domain diameter may be of order[21] 300 A. The filling factor (fractional volume) occupied by framework planar defects is typically $\lesssim 10^{-3}$, while the critical bulk concentration[16] for point defects decorating these framework planar defects is typically $\gtrsim 10^{-2}$. This means that the planar point defect array may be trapped by microtwin pairs of defect framework planes, or merely by the stress field of an antiphase or twin defect framework plane. In any case, the filling factor or concentration associated with the electronic domain wall is at least an order of magnitude larger than that of the framework planar defects observable by electron microscopy.

If the domain walls form a continuous network, then the conductivity will be dominated by the electrical properties of the walls. If the latter are semiconductive, then the material will be macroscopically semiconductive, even though the domains remain metallic. Now suppose we change the processing to reduce the point-defect concentration. As mentioned above, the most likely possibility is that when the metal-insulator transition occurs, the electronic walls do not disappear. Instead, when the average length of the framework walls exceeds a critical value, gaps appear in the electronic defect densities which make the electronic walls semiconductive, and the electronic wall network is discontinuous, as shown in Fig. 2, with metallic bridges or shorts in the gaps. If the size of these gaps is small compared to the bulk electronic mean free path, carrier scattering by the walls of the weakly metallic channels formed by the gaps will dominate scattering in the metallic domains, and most of the momentum dissipation will occur at the walls or edges of the narrow channels formed by the gaps in the defect density of the domain walls. Note that these electronic gaps can form even though the framework twin or antiphase walls themselves remain continuous, so that the topology of $N(E_F,\mathbf{r})$ is hidden from electron microscopy. At the same time the composition at which the electronic gaps form is implicitly associated with a geometrical (more accurately, topological) singularity which represents a percolative threshold both electronically (for electrons near E_F) and structurally (because the electrons near E_F are the ones that are most easily polarized to screen long-range elastic forces). Moreover, this is the only singularity in the domain-wall model. As is shown in Sec. X, this singularity explains quite well the first-order transition in transport properties which occurs in well-annealed samples $La_{2-x}Sr_xCuO_4$ in conjunction with a second-order structural transformation.

At this point it is helpful to state explicitly what we suppose the effect of the gaps in the domain walls may be on the basis states which are properly used to calculate electrical properties. Suppose $w\lesssim c$, then the number of ballistic states N_b compared to the total number $N_t=N_l+N_b$ of localized and ballistic states should be of order $N_b/N_t\sim c/d$, in other words, N_b tends to zero linearly with c. As a function of chemical composition X, we may expect that c varies linearly above a threshold $X=X_0$, that is, $c\sim|X-X_0|$. This linearity may persist to a number of physical properties [for example, $T_c(x)$],

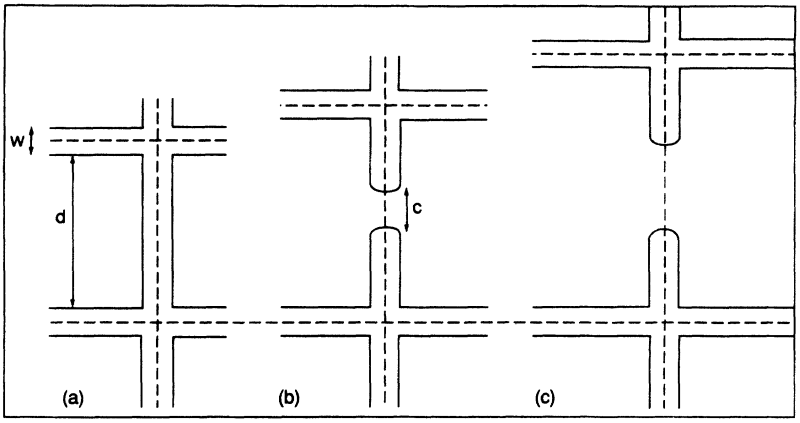

FIG. 2. Domain-wall geometries as a chemical variable X is varied through the metal-insulator transition at $X=X_c$. (a) $X<X_c$, sample insulating. (b) $X=X_c+\varepsilon$, sample has just become metallic with maximum T_c, metallic gaps or channels of width $c\sim w$ appear in the electronic domain walls. (c) Larger gaps appear, but the density of defects in the domains may also increase; that is, the defects may be less concentrated near the walls, and T_c may decrease while ρ increases. The framework defects are shown by dashed lines as isolated planes, but they also form pairs of closely spaced planes (Ref. 18).

and, in any case, it will tend to mask the exponential singularities which occur in bulk homogeneous theories of superconductivity such as the BCS theory.

We can calculate the temperature dependence of the gap-channel resistance as follows. The current-carrying states form wave packets that propagate through the channels. These states are restricted by the exclusion principle to lie in the kT-wide energy range determined by the product $f(1-f)$, where the Fermi factor f is $f=[1+\exp(E-E_F)/kT]^{-1}$. The probability that the packet will scatter off the sides of the channel as it passes through the gap is proportional to the length of the channel and to the number of final states it can scatter into, which is proportional to T. This factor arises here exactly as in Landau theory. However, there is no second factor of T because both momentum and energy are transferred to the wall as whole. (Compare the example of umklapp scattering discussed above, where the umklapp momentum is absorbed by the crystal as a whole.) The latter is temperature independent because the energy and momentum are absorbed not by a single independent second electron, but by many strongly correlated electrons localized in the wall which do not carry current themselves.

Most of the experimental data will be discussed in the following sections appropriate to each class of materials, so that we can analyze chemical trends in detail. However, there is one experiment we wish to discuss here because it illustrates quite neatly the special features of the geometry of extended defects. The resistivity $\rho(T)$ of epitaxial $YBa_2Cu_3O_{7-x}$ films was measured as a function of ion-beam-induced damage.[26] With $\rho(T)=\rho_0+bT$, it was found (as expected) that the residual resistivity ρ_0 increased with fluence ϕ and the originally superconductive films ($T_c\sim 90$ K) become semiconductive for fluences above $\phi_c\sim 20\times 10^{13}$ ions/cm^2, with $d\rho/dT\geq 0$ for $T_c<T<300$ K. Also, T_c ($R=0$) disappeared at about this fluence, as expected.

The surprising result of the damage experiment concerns $b(\phi)$. For $\phi\lesssim\phi_c/2$, the slope $b(T)$ *increases* with ϕ, which is certainly counterintuitive because one would have expected only ρ_0 to increase if the ions created only point defects. However, what actually happens is that the ion leaves a cylindrical damage track with estimated[26] diameter $d\sim 8$ Å, which is significant on a scale of wall width $w\sim 50$ Å, which may also be a good estimate of the channel dimension c [Fig. 2(b)] for samples close to a metal-insulator transition. The fractional increase in b is about equal to ϕ/ϕ_c, although, because of sample inhomogeneities, ϕ_c is not well defined. In any case, these data clearly show that there is a close relation between cylindrical extended defects and the resistivity linearity, which provides strong support for the cylindrical channel or punctured wall model of the origin of resistivity linearity. Qualitatively the increase in slope results from a decrease in the number of current-carrying states in the channel per unit energy. The overall scattering rate at low T increases, of course, because of increases in ρ_0, which result from bulk scattering from damage tracks.

IV. CHEVREL COMPOUNDS $M_yMo_6Ch_{8-z}O_x$

The salient feature of superconductivity in the Chevrel compounds is the drastic effect[27] of oxygen contamination ($x>0$) which long went unrecognized. Even after this was discovered and found to be responsible for triclinic distortions[28] that correlate well[29] with reductions in T_c for $M=$Sn and Pb, for example, or the insulating character[30] for $M=$Ba, many problems remained. The most serious of these was that the observed average triclinic distortion angle δ is very small, $\lesssim 0.5°$. According to the band calculations,[31] a distortion $\delta\gtrsim 10°$ would be required to reduce T_c to 0 or to render the normal state insulating.

We have recently reviewed[32] the Chevrel data in the light of emerging evidence[15,16] of electronic domain walls in the cuprates and found many similarities. The mystery of the small measured value of δ is easily solved because this refers to the domains and not the domain walls. It is

also most interesting that linear temperature dependent $\rho(T)$ is found[33,34] in carefully prepared samples of $PbMo_6S_{8-z}O_x$. Thus, the linear dependence is not a property unique to layered cuprates but is rather associated with covalent-ionic bonding in transition-metal oxides and chalcogenides (especially sulfides).

It is instructive to review the data in detail. In single crystals of $PbMo_{6.2}S_8$ of volume ~ 1 cm^3, $\rho(T)$ is linear[33] from T_c up to 50 K. Linearity at higher T may be masked by inclusions of other phases (Mo_2S_3). Sintered samples exhibit[34] linearity up to 40 K and linearity may be limited for the same reason. But, the most striking result is that oxygen-doped $M=$Eu samples which are insulating as-grown become[35] metallic and superconductive with $T_c \sim 10$ K abruptly at pressures above $P_t \sim 10$ kbar. This transition cannot be explained by hopping models[3] or by any spatially homogeneous model because no structural change is observed by diffraction. We suggested[32] that, at this transition, the semiconductive domain walls fracture and the metallic domains become metallically connected along the fracture lines. This is analogous to the channels formed in Fig. 2(b) compared to the semiconductive domain wall array of Fig. 2(a). It seems very unlikely that, at these modest pressures, the domain walls could have disappeared completely. Moreover, by growing $M=$Eu samples in the presence of an oxygen getterer, superconductivity is achieved[27] at $P=0$, which means that the semiconductive behavior of the as-grown samples[35] is almost surely caused by oxidized domain walls. Similarly, the degradation of T_c as the oxygen content increases probably indicates the gradual narrowing of the channels in Fig. 2(b).

V. PEROVSKITE SUPERCONDUCTORS (K,Ba)(Pb,Bi)O_3

The family $Ba(Pb,Bi)O_3$ exhibits superconductivity with T_c up to ~ 15 K, while in $(K,Ba)BiO_3$ the value of T_c can be as large as 30 K. One of the most striking aspects of superconductivity in this family is that T_c varies smoothly through the maximum $T_c \sim 15$ K in $Ba(Pb,Bi)O_3$, with the likelihood of at least short-range (Pb,Bi) sublattice ordering at the optimal $Pb_{0.75}Bi_{0.25}$ composition.[36,37] However, at the same time, in $Ba_{1-x}K_xBiO_3$, as x decreases, T_c increases to its maximum value at $x=x_c=0.37$, whereupon a metal-insulator transition occurs.[38] We expect that the latter is associated with a large lattice instability, but what is actually observed is only a small rhombohedral distortion δ of the cubic superconductive perovskite.[38] The value of δ at the transition was too small to measure, but was probably less than 0.2°. According to band theory,[39] this should not produce a metal-insulator transition, but even if this happened by accident, the resulting energy gap would be $\lesssim kT$ at room temperature and the material would still be metallic.

This behavior is strikingly similar to that observed for $BaMo_6S_8$, and sample quality permitting, one would expect that insulating $Ba_{1-x}K_xBiO_3$ with $x<0.37$ should become metallic abruptly with increasing pressure, as $EuMo_6S_8O_x$ did.[30] In any case, with such small rhombohedral distortions the only viable explanation for the metal-insulator transition is domain walls. One would also expect that well-annealed samples would exhibit a linear $\rho(T)$, but even after extensive annealing in oxygen to reduce the oxygen vacancy concentration,[40] superconductive $(Ba,K)BiO_3$ alloys are weakly semiconductive ($d\rho/dT<0$) for $T>T_c$. This means that the bulk mean free path is too short for scattering from the domain walls to be significant.

A determined effort has been made with EXAFS to measure[41] the atomic displacements associated with the metal-semiconductor transition in $Ba(Pb,Bi)O_3$ and $(Ba,K)BiO_3$. This is a difficult experiment because, in general, EXAFS lacks the spatial resolution needed to resolve the clustering effects which lead to domain-wall formation. However, the results are quite interesting, especially when compared[41] with measurements of the optical gap ($E_g \sim 2$ eV in $BaBiO_3$). The slope dE_g/dx is greatest at the metal-semiconductor transition near $x=x_c=0.37$ in $Ba_{1-x}K_xBiO_3$, while the long-short Bi-O distance difference appears to be ~ 0.15 Å at the transition. As remarked above, much larger distance differences are needed to account for $E_g \sim 2$ eV, so the explanation of insulating domain walls seems appropriate. This is topologically different from other models[41] of spatial inhomogeneities in the sense that here the defects are clustered to form a continuous network.

VI. LAYERED CUPRATES

The most spectacular linear resistivity $\rho_{ab}(T)$ in the layered cuprates is obtained for $Bi_{2+x}Sr_{2-y}CuO_{6+\delta}$ crystals[3,4] with $T_c \lesssim 10$ K. Unlike the Chevrel compounds, secondary phases can be almost completely excluded. Also, the CuO_2 plane is very stable up to 700 K. At the same time, T_c is low because the CuO_2 planes are separated by four semiconductive (Bi,Sr) oxide layers. There are various theories concerning why large interlayer interactions are necessary for high T_c, but most of them are electronic and assume sample homogeneity. However, if one accepts the ubiquity of domain walls in the CuO_2 planes, then defect-generated interlayer coupling provides alternative metallic and superconductive paths which may substantially enhance T_c in materials like $YBa_2Cu_3O_{7-x}$ and the bismates and thallates with several CuO_2 planes per unit cell. This is the basis of the quantum percolation model[42] of T_c enhancement in multilayer cuprates where the CuO_2 or CuO planes are separated by only one or two semiconductive oxide layers. When there are four such layers, interlayer coupling is very weak and interdomain coupling is expected to occur primarily through gaps or channels in the intralayer domain walls.

Superconductive samples of $Bi_{2-x}Sr_{2+y}CuO_{6+\delta}$ have been prepared in two ways.[3,4] Polycrystalline (ceramic) samples were formed by repeated sintering.[4] With these samples with nominal compositions $x=y$, by varying x one passes through the metal-semiconductor transition and obtains superconductivity with a linear normal-state resistivity, as shown for the reader's convenience in Fig. 3. The room-temperature resistivity is lowest and T_c is

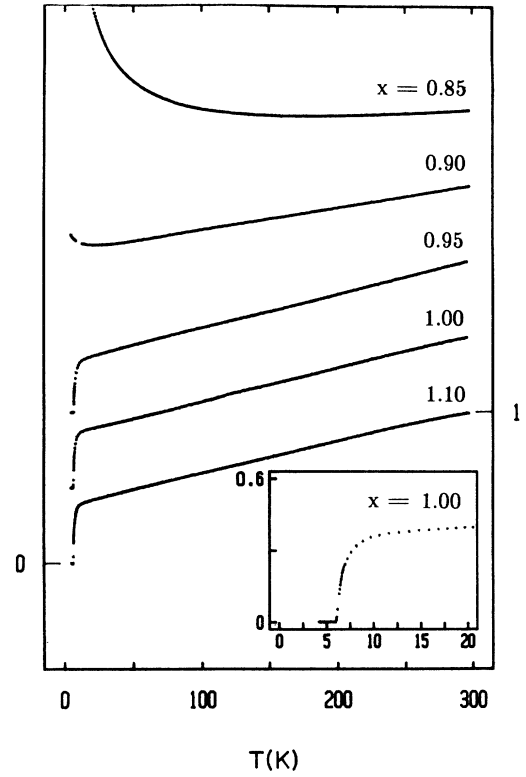

FIG. 3. Resistivity $R(T)$ against temperature for a series of $(Bi_{2-x}Sr_x)_2CuO_{6+\delta}$ polycrystalline samples with variable x, as reported in Ref. 2 and reproduced here for the reader's convenience.

maximized just at the metal-insulator transition,[4] again shown for convenience in Fig. 4. For larger Sr content it appears that the electronic defects no longer concentrate so effectively near planar framework defects.

We can understand this behavior if we assume that in the superconductive phase the high-T_c region consists of a sheath of thickness of order $w < d$ bound to the domain-wall-domain interface. As Sr content increases,

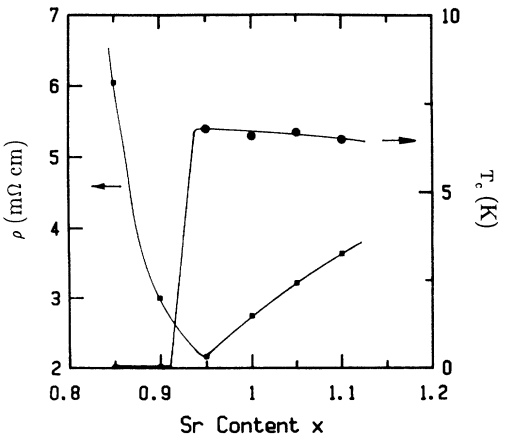

FIG. 4. Room-temperature resistivity for the samples of Fig. 3, together with T_c ($R=0$), as reported in Ref. 2 and reproduced here for the reader's convenience. Note that the dominant chemical parities of ρ and T_c are, respectively, even and odd.

the defects no longer concentrate so effectively near the twin and/or antiphase domain planes. This reduces c_i and with it T_c. However, the concentration of defects in the domains may still increase, thus increasing the bulk resistivity and ρ(297 K).

It is important to realize that, however complex this inhomogeneous model may seem, it is extremely difficult to explain the results shown in Fig. 4 with a homogeneous model. This is because in such a model inevitably T_c and ρ(297 K) should be related over a narrow range of compositions, but it is clear that such a single-valued relation cannot be found to describe T_c (nearly a step function, which is odd about $x = x_c$) and ρ(297 K) (a "V" which is nearly even about $x = x_c$). This is why no mention is made of the metal-insulator transition itself in the homogeneous or "Fermi-liquid" models of the linearity of $\rho(T)$ discussed in the next section. Another way of making the same point is to observe that, in a one-component model, the functional relationship between T_c and ρ must be an even function of $(x - x_c)$, but in a two-component model it can be an odd function. Since $T_c(x - x_c)$ is mainly odd and $\rho(x - x_c)$ is mainly even (Fig. 4), any successful model must contain at least two components.

Because it is so important, we expand on this point in Fig. 5. Suppose in a Fermi-liquid model as the composition X is varied that E_F varies and $N(E_F)$ increases while the electron-whaton coupling is nearly constant. (A whaton may be a phonon, a spin wave, a plasmon, an exciton, or what have you, and we assume that the same strong coupling, directly or indirectly, is somehow responsible for the temperature dependence of the resistivity and for Cooper pair formation. This is certainly the case for phonons, and it is assumed to be the case for other whatons in exotic theories.) Then both $T_c(X)$ and $\rho(X)$ will vary

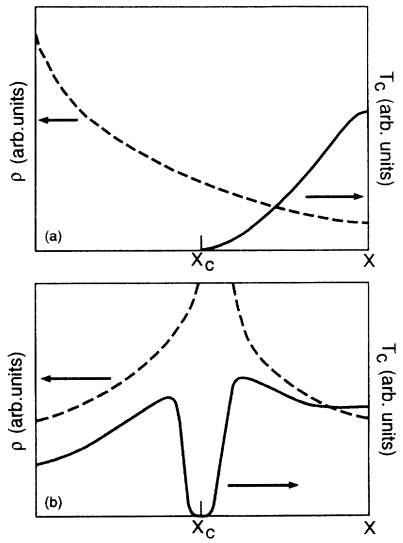

FIG. 5. Sketches of possible patterns for ρ(300 K) and T_c as a function of chemical variable X in homogeneous Fermi-liquid models, (a) without nesting instabilities such as spin- or charge-density waves, and (b) with such instabilities. Note the common dominant chemical parity of ρ and T with respect to $X - X_c$ in both cases, which is characteristic of one-component (homogeneous) Fermi-liquid theory.

monotonically as X is varied, and the general trend will be that shown in Fig. 5(a). The dominant chemical parities (DCP) of both T_c and ρ with respect to $x-x_c$ are odd.

A second reasonable possibility, at least for the layered cuprates (but not for three-dimensional Chevrel compounds or NbO_x) is that, at $X=X_c$, the Fermi surface is nested, with $E=E_F$ at a logarithmic peak in $N(E)$ generated by a two-dimensional saddle point. Then one can have charge-density waves (CDW), spin-density waves (SDW), or a high-T_c superconductor.[43] In this case the behavior of $T_c(X)$ and $\rho(X)$ is shown in Fig. 5(b). Neither T_c or ρ will follow $N(E_F)$ if CDW or SDW form because of the nesting condition. In this case both DCP's are even.

With the possible exception of $(La,Sr)_2CuO_4$, no high-T_c superconductor follows a general trend resembling either Fig. 5(a) or 5(b). However, all of them exhibit linearity in $\rho(T)$ which correlates well with high T_c. The common feature of Figs. 5(a) and 5(b) is that, whether or not there is an alternative electronic instability which upsets the functional relations between T_c and ρ, and $N(E_F)$, the DCP of T_c and ρ relative to $X-X_c$ remains substantially the same. This is an inevitable consequence of sample homogeneity. The large difference shown in Fig. 4—practically opposite DCP's for T_c and ρ—demonstrates unequivocally that the linearity in $\rho(T)$ cannot be explained by homogeneous one-component Fermi-liquid theory. At least two structural components are needed to produce DCP reversal.

There is one other important point to be made concerning the $(Bi,Sr)_4CuO_{6+\delta}$ system. In the ceramic samples,[4] x [the (Bi,Sr) mixture variable] was tuned through the metal-semiconductive transition, but in the single-crystal samples[1] the relevant variable for obtaining superconductivity was found after extensive searches to be a combination of x and δ, which led to the statement[3] that "the structure of a crystal grown under specific conditions cannot be easily asserted." According to our present model, this variability is due to the difference in ferroelastic clamping constraints between the two kinds of samples and is in itself strong evidence for the need for a multicomponent structural model.

VII. HOMOGENEOUS FERMI-LIQUID MODELS

There have been several efforts in the literature to derive the linearity of $\rho_{ab}(T)$ in the layered cuprates from a homogeneous Fermi-liquid model. I believe that only one of these is mathematically consistent, and this is the marginal Fermi-liquid model.[44] This model is interesting because it shows how unphysical the consequences of homogeneity are in this context. Notably the model predicts that $N(E)$ vanishes logarithmically at $E=E_F$, a condition which is scarcely likely[45] to generate high T_c's. This result can be viewed as the result of taking a kind of harmonic average of Figs. 1(d) and 1(w), and it is the antithesis of Fig. 1(i), which produces high-T_c superconductivity. No attempt is made in this model to discuss chemical trends or to explain the metal-insulator transition. However, this can be done, at least schematically, by replacing $|E-E_F|$ with $[(E-E_F)^2+E_g^2]^{1/2}$, where E_g is the insulating gap which varies like $|X-X_c|$ for $X<X_c$ and is zero for $X>X_c$. With constant electron-whaton coupling one then obtains $T_c(X)$ and $\rho(X)$ patterns similar to those shown in Fig. 5(a). These clearly disagree with experiment.

In earlier papers[45,46] I attempted to explain the linearity of $\rho(T)$ in a two-component context but without specifying the spatial details of the model. Certainly these papers were on the right track in the sense that the two components were extended and localized states, with the dominant scattering of the former due to the latter. However, the model required several assumptions that are now seen to be unnecessary (a linear density of localized states near E_F, elastic extended-localized scattering). In fact, the present two-component model derives the linearity in T of $\rho(T)$ in much the same way as Landau derived the T^2 factor for a one-component Fermi liquid; that is, from phase-space considerations alone. As we have seen, $\rho(T)-\rho_0 \propto T$ is very common in anionic metals, including some which are not superconducting (NbO_x), provided they are vicinal to an inhomogeneity boundary. This makes the derivation given here particularly satisfying.

VIII. HALL-EFFECT ANOMALIES

Many experimental papers have reported anomalies in the Hall resistivity $R_H(T)$ in $YBa_2Cu_3O_{7-x}$ and other layered cuprates. Because of the large uniaxial anisotropy of $\rho_{ij}(T)$ such measurements are more complicated than those of ρ_{ij} itself, because R_H is obtained by inverting the $\sigma_{ij}(H)$ matrix.[47] However, it seems unlikely that these anomalies are artifacts because many workers have reported similar anomalies, especially in layered cuprates. Moreover, the temperature dependence of $\rho(T)$ is similar in single crystals[4] [where $\sigma_{ab}(T)$ is linear] and polycrystalline samples[3] [where an average of $\rho_{ab}(T)$ and $\rho_{cc}(T)$ is measured, but $\rho_{cc}(T)$ is slowly varying].

The present model suggests that these anomalies arise from field-induced carrier freeze-out (or localization) on extended linear or planar electronic defect arrays. Because these arrays are native defects generated by internal misfit in the layered unit cell, we expect to see several kinds of extended defect arrays in each material. However, the specific defects that arise, twins, microtwins, antiphase planes,[23] spiral growth defects,[48] mixtures of a-axis with c-axis domains in thin films,[49] or what have you, will vary according to the geometry and method of sample preparation.

Localization or magnetic freeze-out near a $d=$ three-dimensional metal-insulator transition is observed[50] for randomly distributed impurity centers in Si:P. When the point defects are concentrated near a $\tilde{d}=1$ (linear) or $\tilde{d}=2$ (planar) framework, magnetic localization can occur much more abruptly as a result of the reduced dimensionality $d'=d-\tilde{d}$ of the degrees of freedom normal to the framework, $d'=2$ or 1 in the linear or planar cases. An arbitrarily weak attractive short-range potential always produces localization for $d'=1$, but for the $\tilde{d}=0$ (point defects only) case, $d'=d=3$, and there is a

threshold strength for producing bound states. The most interesting case is $d'=2$, which is marginal and has been discussed by scaling theory.[51] Note that magnetic freeze-out is itself a consequence of the partial dimensional reduction associated with an applied field, which confines electron motion normal to the field. Reductions in dimensionality (or more generally, degrees of freedom) always favor localization.[51] Averaging over the wide variety of possibilities of reduced dimensionality in general we would expect to find that localization will always contribute a Hall voltage linear in the applied magnetic field and that this will be the dominant contribution in the normal state for small fields. If a large enough number and variety of extended defects are involved in localization, then this should be linear in temperature as well. Exceptions may arise in samples where a single type of extended defect is dominant, for then a magnetic freeze-out temperature characteristic of that defect may be observable.

The nature of the freeze-out is rather subtle and it depends explicitly on the spatial dependence of $N(E)$ shown in Fig. 1. According to this figure, $N(E_F)$ reaches its maximum value just at the interface between the domain wall and the domain. This is the region where the usual Bohr–van Leuuven skipping boundary orbits[52] are formed. In their classical model of diamagnetic susceptibility these skipping orbits cancel the contribution of the internal cyclotron orbits, leaving zero orbital diamagnetism. Normally it is assumed that this cancellation does not occur because the scattering rate for the boundary orbits is much larger than that for the internal orbits. However, in the present case these orbits may be coherent over large distances. This would facilitate localization on the extended defects (domain walls) at low T. The phase coherence of the boundary orbits can be quenched by impurity scattering, which would thereby suppress freeze-out.

These qualitative ideas can be made more quantitative in the context of Fig. 2. When freeze-out occurs the magnetic orbits are separated into the boundary orbits and the orbits localized in single domains. The boundary orbits are assumed to carry no Hall current. The latter is carried by thermally activated hopping of carriers between adjacent domains. In each domain the Landau levels contain a single level E_n closest to E_F, with the average value of $|E_n-E_F|=\alpha\hbar\omega_c$, where $\alpha=\frac{1}{2}$ and $\omega_c=eH/m^*c$. The average activation energy is thus $\alpha\hbar\omega_c$, and for small H the Hall voltage V_H will be proportional to $\hbar\omega_c/kT$, or the hall resistance R_H will be proportional to T^{-1}; that is, $n_H \propto T$. In thermally activated films with complex defects such that a large fraction f of V_H is concentrated on one defect, the relevant factor may be feV_H/kT, which is not small, and more rapid freeze-out may be observed.[47] With Zn doping the boundary orbits are mixed with the localized Zn orbits and freeze-out is suppressed.[16]

The experimental data for R_H for $\mathbf{B}\perp$ nominal c axis of films and single crystals are consistent with this discussion. Early work[47] on uncharacterized epitaxial films of $YBa_2Cu_3O_{7-\delta}$ grown on unheated substrates showed a wide range of behavior for the carrier density $n_H(T)$ defined as $(R_He)^{-1}$, including abrupt freeze-out for the "poor" films with lowest critical current j_c and linear freeze-out for the "best" film with the highest j_c, which presumably had the lowest concentration of extended defects. Single-crystal measurements[53] showed $n_H(T)$ linear. In all cases the best material showed the smallest values of $n_H(293\ \mathrm{K})$, and the smallest range between 150 and 100 K. Recently measurements[54] on highly oriented epitaxial films of $YBa_2Cu_3O_{6.9}$ showed weak freeze-out with an S-shaped $n_H(T)$ saturating near 100 K at about 0.5 carriers/unit cell, and saturating near 300 K at about 1.0 carrier/unit cell. These samples have apparently the lowest concentration of extended defects of any samples studied so far. The rapid upturn of $n_H(T)$ generally observed below $T_u \sim 150$ K occurs only below $T_u \sim 100$ K in these samples. This upturn is often ascribed to dynamical fluctuations, but it is almost surely associated with static superconductive "patch" effects and variable oxygen stoichiometry in the neighborhood of extended defects, even in single crystals.[55]

One of the interesting questions is which point defects are responsible for these Hall anomalies. The most plausible candidates are the oxygen vacancies in the CuO_{1-x} chains because these are the point defects whose concentration changes the most during the oxidation process which generates internal stress and extended defects. This hypothesis can be tested by examining $R_H(T)$ for $YBa_2Cu_4O_8$, grown[56] under high O_2 pressure and annealed for 72 h at 1025 °C in 95 bar O_2. In this case $n_H(T)$ is constant above 150 K (no carrier freeze-out), but exhibits linear freeze-out below 150 K, with no upturn approaching T_c. Thus, these samples may be quite homogeneous with perhaps a high density of clusters of point defects, but with few extended defects or superconductive patches.[57] Similarly, the temperature-independent Hall coefficient found[58] in sintered $La_{2-x}Sr_xCuO_4$ probably reflects the absence of extended defects in this material, where there is only one CuO_2 plane and the YBCO problem of lattice-constant mismatch between CuO_2 and CuO_{1-x} planes does not arise.

The nature of carrier freeze-out can be probed in sintered $YBa_2(Cu_{1-y}Zn_y)_3O_{7-x}$. There Hall measurements show[59] that, as y increases, freeze-out is suppressed. This is what we would expect on the basis of the above discussion of impurity disruption of the phase coherence of Bohr–van Leuuven boundary states. Because Zn stains the domain walls,[16] it is particularly effective both in reducing T_c and suppressing Hall carrier freeze-out.

Another interesting example which supports the present model of extended defects generated by internal stress is $Pr_{0.5}Ca_{0.5}Ba_2Cu_3O_{7-\delta}$. In principle, this alloy is isovalent to $YBa_2Cu_3O_{7-\delta}$ because the respective valences $(+z)$ are Pr(+4), Ca(+2), and Y(+3). In practice, it has not proved possible to grow bulk samples of $Pr_{0.5}Ca_{0.5}Ba_2Cu_3O_{7-\delta}$ which are superconductive, but 300-nm epitaxial films prepared by laser ablation are superconductive[60] with $T_c \sim 40$ K. The absence of bulk superconductivity can be explained[60] in several ways in terms of point defects (larger bulk δ, for example), but all

of these explanations involve drastic chemical changes in relatively thick (> 300 nm) films. The basic point about internal stress is that it increases with increasing film thickness, as is well known for heteroepitaxial semiconductive films.[61] Thus, in the bulk samples we expect to find semiconductive domain walls which may be absent in the laser-ablated thin films, which are formed so rapidly as to suppress the growth of extended defects. Studies of T_c as a function of film thickness in $Pr_{0.5}Ca_{0.5}Ba_2O_{7-\delta}$ indeed should provide the best test for the present structural model, with an abrupt decrease in T_c beyond a critical thickness.[61] Point-defect models, on the other hand, would predict a more gradual decrease in T_c, especially since the thicker films would still in the point-defect model be expected to have a superconductive surface layer $\sim$300 nm thick.

The question of inhomogeneities has been addressed in a non-Fermi-liquid context by Mott, using a homogeneous bipolaronic hopping model.[62] With several flexible assumptions he is able to derive the T linearity of ρ_{ab} and n_H in $YBa_2Cu_3O_{7-x}$. He then invokes disorder to explain the constancy of n_H in sintered $La_{2-x}Sr_xCuO_4$. This naturally leads him to the prediction that, with ion damage or with increasing x in $YBa_2Cu_3O_{7-x}$, the carrier density $n_H(T)$ should lose its linearity in T and become constant, which is opposite from the behavior actually observed.[26,54] I agree with Mott that disorder is present, but in my model the samples are never truly homogeneous. The differences between materials, or even between the same material in samples with similar T_c's but different normal-state transport characteristics, arise primarily from differences in defect topologies, clustered, continuous, or discontinuous extended. In any event, in spite (or perhaps because) of mathematical simplicity, homogeneous models appear to achieve the maximum distance from experiment.

IX. CORRELATION OF T_c AND LINEAR BACKGROUND TUNNELING CONDUCTANCE IN (K,Ba)(Pb,Bi,Sb)O_3 SUPERCONDUCTORS

One of the striking characteristics which distinguishes anionic (oxide) superconductors from metallic superconductors is the presence of a background conductance which scales linearly with voltage over a large voltage range (-0.2–0.2 V or more). This linear background conductance has recently been studied systematically[63] for four groups of superconductive perovskites ($BaPbO_3$, $BaPb_{0.75}Sb_{0.25}O_3$, $BaPb_{0.75}Bi_{0.25}O_3$, and $Ba_{0.7}K_{0.3}BiO_3$) with T_c varying from <1 to 30 K. It was found that the slope of the linear conductance was approximately proportional to T_c. Because we have at present no reliable independent means for estimating such trends in T_c, this observation is remarkably interesting. In fact, it can be explained quite simply in the context of spatial inhomogeneities.

To begin we must first have a model which explains the linearity (which is almost exact) of the conductance against voltage. It is clear that a linear conductance is different from a linear resistivity, and thus it would seem at first sight that the structural explanation used for the linear resistivity in Sec. III cannot be applied here to discuss the linearity of the background conductance. In fact, there is a close connection between the two because the linear resistivity corresponds to Fig. 2(b), while the linear conductance corresponds to Fig. 2(a). In other words, the linear resistivity is found just on the metallic side of the metal-insulator transition, while the linear conductance is found just on the insulating side. The compositional difference between the two sides is small and this is what makes possible the systematic correlation of the slope of the normal-state background tunneling conductance with T_c.

Linear (in T or frequency or voltage) conductances have previously been observed[64] in two semi-insulating contexts, lightly compensated semiconductor impurity bands, and stable quasicrystals, such as *i*-Al-Cu-Fe. Again the linearity is excellent and, in the quasicrystal case, it extends up to $\hbar\omega \sim 1$ eV; that is, well above the Debye energy, $k\theta_D \lesssim 0.05$ eV. I have explained[65] this linearity in terms of a fixed- (not variable-) range hopping model which I call compartmentalized. With a specific structural model[66] for *i*-Al-Cu-Fe, I was able to identify a pseudogap in the electronic spectrum of 1 eV, and it appears that this gap explains the 1-eV cutoff of the linear conductance observed[64] for Al-Cu-Fe. The slope of this conductance appears to be the same[67] in *i*-Al-Cu-Li as in *i*-Al-Cu-Fe, although I predicted that a smaller cutoff ($\sim$0.3 eV) should be observed for the former.

Within two-component Fermi-liquid theory,[68] one can easily distinguish between materials on the metallic and insulating sides of a metal-insulator transition. The density of states at the Fermi energy $E = E_F$ is written as

$$N(E_F) = N_b(E_F) + N_d(E_F) , \tag{1}$$

where $N_b(E_F)$ describes extended states which carry current quasiballistically (quasi-Bloch states), while $N_d(E_F)$ refers to localized or standing-wave states. The latter are phase incoherent from one domain to the next, and interdomain current is carried by classical hopping. In this case the diffusivity D is proportional to T^2 while the mobility μ is given by the Einstein relation

$$\mu = D/kT \tag{2}$$

so that the conductance $\sigma = e^2\mu$ is proportional to T. Alternatively, kT, which determines the width of the Fermi function, can be replaced by $\hbar\omega$ for optical conductance or by eV for tunneling conductance. In each case we obtain a linear conductance. Note that, if the hopping range is dynamically variable in any way, this linearity will be lost.[65,65] The static range in the present model is simply the average spacing of domain centers, and the domains themselves are the compartments which define the localized states.

With these physical analogies we have a firm basis for understanding linear conductances, so we can now consider the slope of this conductance. The range of slopes observed experimentally is only an order of magnitude, so that we need not try to explain exactly why T_c appears to be proportional to the slope. We must, however, explain why both increase together. Compartmentalized hopping

takes place over barriers (domain walls), and the barrier height is related to the cutoff for the linearity of the conductance.[65]

To proceed further we need a more explicit structural model. In the barriers we assume that $N_b(E_F)=0$; that is, we are on the insulating side of the metal-insulator transition. On the metallic side, $N_b(E_F) \ll N_d(E_F)$; that is, most of the states are localized, and in a two-component expression for the electron-phonon coupling constant,

$$\lambda=\lambda_b+\lambda_d=N_b(E_F)V_b+N_d(E_F)V_d \ , \tag{3}$$

we still have $\lambda_d \gg \lambda_b$. Thus, T_c will be determined primarily by λ_d, not λ_b, and this is why a correlation between T_c and the conductance slope is possible.

It is important to realize that the localized states should be described not as self-trapped polarons but rather as domain-wall-pinned polarons.[69] The stronger the electron-phonon coupling λ_d, the more effective the pinning. As kT, $\hbar\omega$, or eV increase, the pinning decreases, and this reduced pinning frees more carriers to act as quasiextended current-carrying states. Thus, the slope of the conductance increases with λ_d, as does T_d, so we can now see why the slope is positively correlated with T_c, which was our main purpose. Thermally activated hopping also explains the linearity in T of the Hall conductance, as noted in the proceeding section.

There is one other systematic correlation which is also interesting. Over a factor of 10, the slope of the conductance is linearly correlated with the zero-bias conductance.[26,63] Thus, the latter is intrinsic and also represents a common microscopic factor for the four systems studied. My candidate for this factor is paired BaO-BaO planes [instead of BaO-(Pb,Sb,Bi)O planes as in the crystals]. There are three reasons for this suggestion. First, such stacking faults would make excellent semi-insulating domain walls. Second, they would be common to all four systems studied. Third, in $Ba_{1-x}K_xBiO_3$ with $x \ll 1$ it has recently been observed[70] that K occupies Bi (not Ba) sites, which can be explained as the result of staining of BiO-BiO planes by K (such sites are preferred for electrostatic reasons over crystalline Ba sites). If one can have BiO-BiO stacking faults, then one can also have BaO-BaO stacking faults.

It may be the case that, for an ideal planar geometry, thermal depinning is not linear in T (although this problem seems not to have been solved). However, in reality the domain-wall geometry is far more complex than an infinite plane. Also, the observed range of linearity of the conductance is not large. In the future it may be possible to decide whether the apparently linear relationship between $d^2\sigma/dV^2$ and T_c is real or accidental.

X. RECONCILIATION OF FIRST-ORDER ELECTRONIC WITH SECOND-ORDER STRUCTURAL TRANSITION IN $La_{2-x}Sr_xCuO_4$

One of the primary problems both experimentally and theoretically in understanding the effects of spatial inhomogeneities in cuprate superconductors is that the nature of the inhomogeneities depends on the thermal history of the samples. It may appear that this is not the case because, for example, different methods of sample preparation seem to yield very similar T_c's. However, to obtain similar T_c's these different methods need to optimize the spatial configuration only for some filaments on a scale less than the penetration depth ($\gtrsim 1000$ Å), whereas the domain sizes which have been observed, for instance, by electron microscopy, are considerably smaller ($\lesssim 300$ Å). One way to circumvent this ambiguity is to study the effect of long annealing times on T_c near a well-established structural phase boundary. With long annealing times domain sizes grow and eventually exceed the penetration depth, leading to observable changes in T_c and/or the superconductive volume fraction.

Although this procedure sounds simple in principle, in practice, for oxides it requires exceptional care because the needed annealing times can be very long. The first successful experiment of this type appears to be the study[71] of the superconductive volume fraction in well-annealed $La_{2-x}Sr_xCuO_4$ near the orthorhombic-tetragonal transition at $x=0.21$. For the reader's convenience, these dramatic data are reproduced in Fig. 6. They show a structural transition which is apparently continuous while both the superconductive and normal-state transport properties are discontinuous, with the magnitude of the discontinuity increasing with annealing or improved homogenization (spray-dry samples). The changing volume fraction suggests that the changes in T_c

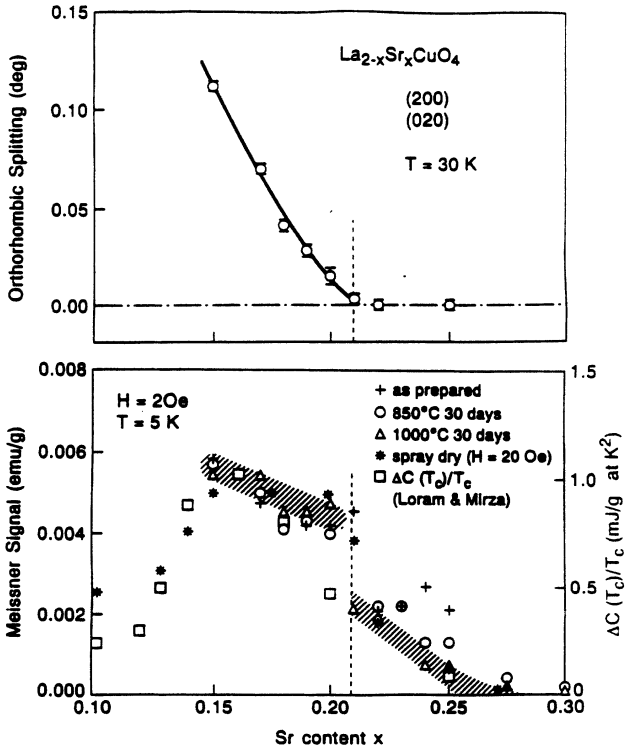

FIG. 6. The effects of the orthorhombic-tetragonal structural phase transition (upper panel) on the volume fraction of superconductive material (lower panel), as reported in Ref. 66. It is likely that the residual superconductive volume above $x=0.21$ is associated with composition fluctuations which produce orthorhombic microdomains.

or the normal-state resistivity temperature index n are associated with quantum percolation of the kind described by the present model. The very small orthorhombic distortion angles ($\lesssim 0.1°$) shown in Fig. 6 also suggest that the distortion itself near $x=0.21$ has a percolative origin, and that it is no longer observable when the tetragonal phase percolates. In a predominantly two-dimensional geometry, of course, only one phase can percolate. For the tetragonal phase this occurs when cracks or metallic channels appear in the domain walls, which is a topological singularity (Sec. II). All percolative transitions are continuous, and the domain size increases as the transition is approached from the orthorhombic side. If we think of the domain walls as pinning an internal soft mode (local tilting of CuO_6 octahedra), then the correlation length for this mode should be very large, even larger than observed[72] for $x \lesssim 0.07$.

I will not comment here on the quantitative details of the experimental results, which are still preliminary. However, there is an important qualitative point. When domain walls are present (orthorhombic phase, or "tetragonal" phase, but inhomogeneous or poorly annealed) both superconductivity and linear T normal-state resistivity are observed. When the domain-wall density is reduced, T_c drops appreciably and the normal-state resistivity is no longer linear in T. These qualitative trends are exactly in accord with the structural model of this paper. As far as I can see, there is no way to explain the (first-order electronic)-(second-order structural) dichotomy within the context of any homogeneous whaton model,[73–75] regardless of the microscopic choice of whatons. As further progress is made in refining phase diagrams with well-annealed samples, I expect that the role of defect ordering, Fermi-level pinning, and extensive structural defects in producing high-T_c superconductivity will be clarified.

XI. INTERLAYER METALLIZATION IN IODINE-INTERCALATED (2:2:1:2)

When the Bi-O layers of (2:2:1:2)=$Bi_2Sr_2CaCu_2O_{6+\delta}$ are intercalated with I, the *ab* planar resistivity ρ_{ab} is virtually unchanged, but the interlayer resistivity ρ_c changes dramatically[76] from semiconductive to exactly linear in T. However, the magnitude of ρ_c remains much larger than ρ_{ab} ($\rho_c/\rho_{ab} \gtrsim 10^3$). This means that the I layer has shorted the semiconductive layers over a small area, with a fractional filling factor $f_c \lesssim 10^{-3}$. These shorts must be of exactly the same type as the channels or shorts which we have introduced to explain the linearity of ρ_{ab} in pristine materials such as other cuprates as well as $PbMo_6S_8O_x$ and NbO_{1+x}.

It is interesting to discuss the microscopic origin of the interlayer defects responsible for the linearity of ρ_c after intercalation. The intercalated iodine layer is found to be epitaxial,[76] but there is no reason that its prototypical lattice constant should match exactly that of the (2:2:1:2) substrate. (Typically, successful intercalation is possible when the lattice constants match to within a few percent.) We therefore expect that the intercalated iodine forms islands, with their centers staggered from one BiO layer pair to the next. When the edges of these islands cross (in projection along the c axis), a large stress is exerted on intervening Bi-O and Sr-O layers which may, for example, attract interstitial oxygen to the crossed regions. If the diameters R of the iodide islands are of order $R/a \sim 30$ (where $a \sim 5$ Å is the *ab* planar lattice constant), then the filling factor of the crossed regions will indeed be of order $f_c \sim 10^{-3}$. A value of $R/a \sim 30$ is consistent with a misfit of prototypical lattice constants of order 1%.

The preceding structural model was presented to facilitate visualization of the kind of defect reconstruction which is needed to explain both the linearity and magnitude of ρ_c after intercalation. However, it is important to realize that this is just an example. What are much more important are the general principles behind the specific model. To explain the data, a small filling factor is necessary and this small filling factor is associated with hidden defects which cannot be imaged by diffraction or by electron microscopy. Moreover, these defects generate a linear resistivity ρ_c which must arise in much the same way as the linear resistivity ρ_{ab}. Thus, the latter also depends on defects or shorts through semiconductive domain walls. This means that the observed linearity of ρ_c and the small value of f_c provide decisive evidence in favor of the structural model of this paper, as well as decisive evidence against homogeneous models of any kind for the linearity of $\rho(T)$ for any material.

In conclusion, we have seen that spatial inhomogeneities can drastically affect the normal-state transport and superconductive properties of metallic oxides vicinal to metal-insulator transitions. The present model not only provides mechanisms which explain linear temperature dependences of planar resistivities and Hall carrier densities, but it also explains chemical trends across either a superconductive metal-insulator transition (Fig. 4) or a superconductive metal–normal-metal transition (Fig. 6). It is noteworthy that the latter exhibits only a second-order structural transition, while the nature of the structural changes for the former is at present still unclear.

The case of $La_{2-x}Sr_xCuO_4$ (Fig. 6) is probably better understood structurally than the other cases discussed here. The decisive factor is domain-wall gettering of Fermi-energy pinning defects. It was suggested some time ago[77] that domain walls might play an important part in high-temperature superconductivity, but the defect-gettering mechanism, together with local enhancement of $N(E_F)$, was not included in the discussion. This mechanism is much more effective than lattice softening of domain-wall phonons, as the phase-space weighting factor[77] of the latter is small.

One can view electronic defect gettering by extended atomic planar defects as a kind of self-organized enhancement of electron-phonon interactions. There may be several kinds of electronic defects, only one of which actually enhances $N(E_F)$ locally. The stress field of the planar atomic defects may attract the electronic defects at longer distances and repel them at shorter distances, leading for each kind of electronic defect to a planar layer at a different average distance from the atomic planar de-

fect. This will produce one high-T_c superconductive layer which can be connected along a channel or crack in the atomic domain wall to the next domain. The mechanism is quite general and merely requires processing optimization, which is customary procedure for these materials and in a deeper sense is implicit in the selection of specific compounds.

Defect chemistry is extremely complex, even in simple crystals like GaAs. For the more complex cuprates one cannot expect to obtain direct evidence in a single experiment to specify all the details of a microscopic electronically decorated domain model. The reader should note, however, that such evidence is gradually accumulating in careful studies of cuprates. Another example of such work is an elastic relaxation measurement[78] of $YBa_2Cu_3O_{6+x}$ which shows evidence for CuO_x chain buckling and (anti)ferroelectric domain formation which is fully compatible with the microscopic model described here.

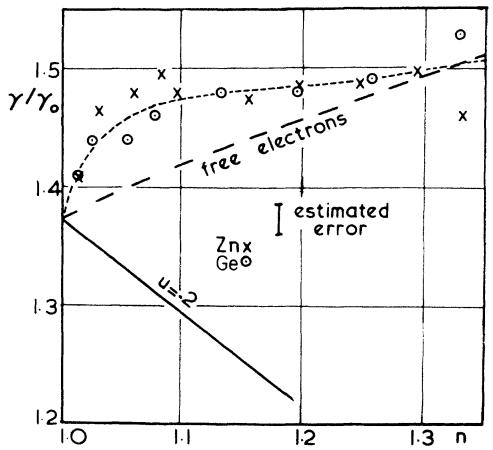

FIG. 7. Variation of reduced electronic specific heat coefficient γ in $Cu_{1-x}Zn_x$ and $Cu_{1-y}Ge_y$ alloys as a function of $n-1=x$ or $y/3$, from Refs. 82 and 83.

XII. FERMI-LEVEL PINNING DEFECTS IN α-BRASS ($Cu_{1-x}Zn_x$) ALLOYS

One of the central theoretical objections usually raised against the present model is that enhancement of $N(E_F)$ by a large resonant defect contribution $N_d(E_F)$ cannot occur because it would be erased by static Jahn-Teller distortions, or with a periodic defect array by charge density waves. I agree that this mechanism is the one that occurs *most* of the time. However, there is no law of nature that says that it must always occur. To prove that such a law does not exist, we need find only one counterexample where Fermi-level pinning by a defect does occur. Unfortunately, as discussed in Sec. II, the likelihood of Fermi-level pinning by defects increases greatly in complex ternary systems where extended defects can be stabilized against Jahn-Teller distortions by cage effects.[79] Nevertheless, I have found an unexpectedly simple example of Fermi-level defect pinning in Hume-Rothery $Cu_{1-x}Zn_x$ (α brass) alloys.

First-principles studies of these close-packed α-phase alloys have shown[80] that Zn dopants form second-neighbor pairs and thus four-member Cu-Zn-Cu-Zn-rings which can be regarded as precursors of the more open bcc β phase. Numerical simulations which reproduce short-range order derived from neutron diffuse scattering intensities[81] are dominated by such pairs even at $x=0.25$.

Long after Hume-Rothery suggested that the $\alpha\rightarrow\beta$ transition was induced by the approach of a nearly free-electron Fermi surface to the (111) or L Brillouin-zone face, Fermi-surface studies showed that there was a large $L_{2'}-L_1$ energy gap at this face, so that the Fermi surface already contacts this fact in Cu- and Ag-based alloys at $x=0$. This means that γ/γ_0, the coefficient of the linear electronic specific heat, normalized to the free-electron value γ_0 at $x=0$, should decrease with increasing e/a (electron-atom ratio). Instead, as Rayne found,[82] it increases, much as if E_F were less than $E(L_{2'})$. His data are shown in Ziman's plot[83] in Fig. 7, reproduced here for the reader's convenience. Also shown is the rigid-band prediction γ_{rb}/γ_0 for a value of $u=|E(L_1)-E(L_{2'})|/E_F$ close to experiment. Note that $d\gamma/dx-d\gamma_{rb}/dx$ is proportional to $N_d(E_F)/x$ in the present model. If $N_d(E)/x$ were independent of e/a, then Fig. 7 would mean that $N_d(E)/x$ was largest near $x=0$. In any case, the large discrepancy between $d\gamma/dx$ and $d\gamma_{rb}/dx$ clearly can be explained only by a Fermi-level resonance associated with Zn pairs. I believe that these Zn pairs are a special case of a defect complex pinning E_F, here in a very simple host (pure Cu). If such pinning can occur in this simple case, I can see no reason why similar pinning should not occur in complex multinary cuprates.

ACKNOWLEDGMENT

I am grateful to S. Martin for drawing my attention to the transport data on NbO_x.

[1]K. M. Rabe, J. C. Phillips, P. Villars, and I. D. Brown, Phys. Rev. B **45**, 7650 (1992).

[2]K. M. Rabe, J. C. Phillips, and P. Villars, Ferroelectrics (to be published).

[3]S. Martin, A. T. Fiory, R. M. Fleming, L. F. Schneemeyer, and J. V. Waszczak, Phys. Rev. B **41**, 846 (1990).

[4]G. Xiao, M. Z. Cieplak, and C. L. Chien, Phys. Rev. B **38**, 11 824 (1988).

[5]A. T. Fiory, S. Martin, R. M. Fleming, L. F. Schneemeyer, and J. V. Waszczak, Phys. Rev. B **41**, 2627 (1990).

[6]R. J. Cava, R. B. Van Dover, B. Batlogg, and E. A. Rietman, Phys. Rev. Lett. **58**, 408 (1987).

[7]S. W. Tozer, A. W. Kleinsasser, T. Penney, D. Kaiser, and F. Holtzberg, Phys. Rev. Lett. **59**, 1768 (1987).

[8]R. Flükiger, R. Baillif, and E. Walker, Mater. Res. Bull. **13**, 743 (1978).

[9]J. A. Wollam and S. A. Alterovitz, Solid State Commun. **27**, 571 (1978).
[10]S. D. Bader and S. K. Sinha, Phys. Rev. B **18**, 3082 (1978).
[11]N. W. Ashcroft and N. D. Mermin, *Solid State Physics* (Saunders, Philadelphia, 1976), p. 346.
[12]K. Kimura *et al.*, J. Phys. Soc. Jpn. **58**, 2472 (1989).
[13]J. C. Phillips and K. M. Rabe, Phys. Rev. Lett. **66**, 923 (1991).
[14]J. G. Allpress, J. V. Sanders, and A. D. Wadsley, Acta Crystallogr. B **25**, 1156 (1969); G. V. Chandrasekhar, J. Moyo, and J. M. Honig, J. Solid State Chem. **2**, 528 (1970).
[15]J. C. Phillips, Phys. Rev. Lett. **64**, 1605 (1990).
[16]J. C. Phillips, Solid State Commun. **81**, 497 (1992).
[17]J. C. Phillips, *Physics of High-T_c Superconductors* (Academic, Boston, 1989).
[18]J. C. Phillips, Phys. Rev. Lett. **59**, 1856 (1987).
[19]J. C. Phillips, (Ref. 17).
[20]R. P. Sharma, F. J. Rotella, J. D. Jorgensen, and L. E. Rehn, Physica C **174**, 409 (1991), see Fig. 7.
[21]M. Ishikawa *et al.*, Solid State Commun. **66**, 201 (1988); see also, M. S. Osofsky *et al.*, Phys. Rev. B **45**, 4916 (1992).
[22]J. C. Phillips, Phys. Rev. B **45**, 5863 (1992).
[23]R. E. Allen and J. D. Dow, Phys. Rev. B **25**, 1423 (1982); C. H. Chen, D. J. Werder, S.-W. Cheong, and H. Takagi, Physica C **183**, 121 (1991).
[24]Z. Tan *et al.*, Phys. Rev. Lett. **64**, 2715 (1990); J. C. Phillips, Phys. Rev. B **42**, 6795 (1990); T. Sakurai *et al.*, Physica C **174**, 187 (1991).
[25]L. T. Romano *et al.*, Phys. Rev. B **44**, 6927 (1991); Y. Zhu, M. Suenaga, J. Tafto, and D. O. Welch, *ibid.* **44**, 2871 (1991).
[26]J. M. Valles *et al.* [Phys. Rev. B **39**, 11 599 (1989)] and K. Winzer and G. Kumm [Z. Phys. B **82**, 317 (1991)] have reported similar correlations of $d\rho/dT$ and ρ_0 for four single crystals of $YBa_2Cu_3O_{6.9}$, all with $T_c=92$ K. These correlations imply that the single crystals contain extended defects similar to those produced in ion tracks.
[27]D. W. Capone, R. P. Guertin, S. Foner, D. G. Hinks, and H. C. Li, Phys. Rev. Lett. **51**, 601 (1983); Phys. Rev. B **29**, 6375 (1984).
[28]D. G. Hinks, J. D. Jorgensen, and H. C. Li, Phys. Rev. Lett. **51**, 1911 (1983); Solid State Commun. **49**, 51 (1984).
[29]R. Flükiger and R. Baillif, in *Superconductivity in Ternary Compounds I,* edited by O. Fischer and M. B. Maple (Springer, Heidelberg, 1982), p. 113.
[30]R. Baillif, A. Dunand, J. Muller, and K. Yvon, Phys. Rev. Lett. **47**, 672 (1981).
[31]H. Nohl, W. Klose, and O. K. Andersen, in *Superconductivity in Ternary Compounds I,* edited by O. Fischer and M. B. Maple (Springer, Heidelberg, 1982), p. 165.
[32]J. C. Phillips, J. M. Vanderberg, and K. M. Rabe, Europhys. Lett. **18**, 349 (1992).
[33]R. Flükiger, R. Baillif, and E. Walker, Mater. Res. Bull. **13**, 743 (1978).
[34]J. A. Woolam and S. A. Alterovitz, Solid State Commun. **27**, 571 (1978).
[35]C. W. Chu *et al.*, Phys. Rev. Lett. **46**, 276 (1981); D. W. Harrison *et al.*, *ibid.*, 280 (1981).
[36]W. Reichardt, B. Batlogg, and J. P. Remeika, Physica B **135**, 501 (1985).
[37]T. Hikata *et al.*, Phys. Rev. B **36**, 5578 (1987).
[38]L. F. Mattheis, E. M. Gyorgy, and D. W. Johnson, Jr., Phys. Rev. B **37**, 3745 (1988); R. J. Cava *et al.*, Nature **332**, 814 (1988); S. Pei *et al.*, Phys. Rev. B **41**, 4126 (1990).
[39]L. F. Mattheis and D. R. Hamann, Phys. Rev. B **28**, 4227 (1983).
[40]B. Dabrowski *et al.*, Physica C **156**, 24 (1988).
[41]J. B. Boyce *et al.*, Phys. Rev. B **44**, 6961 (1991).
[42]J. C. Phillips, Phys. Rev. B **41**, 8968 (1991).
[43]J. E. Dzyaloshinski, Pis'ma Zh. Eksp. Teor. Fiz. **46**, 97 (1987) [JETP Lett. **46**, 118 (1987)].
[44]C. M. Varma, P. B. Littlewood, S. Schmitt-Rink, E. Abrahams, and A. E. Ruckenstein, Phys. Rev. Lett. **63**, 1996 (1989).
[45]J. C. Phillips, Phys. Rev. B **41**, 8968 (1990). The marginal Fermi-liquid model is stated abstractly. However, its key feature is the logarithmic node of $N(E)$ at $E=E_F$, and an explicit example is known which exhibits this analytic singularity. This is the free-electron gas in the Hartree-Fock approximation [unscreened Coulomb interaction, see E. Wigner and F. Seitz, Phys. Rev. **4**, 804 (1933); **46**, 509 (1934)]. The singularity is, of course, removed by dielectric screening due to electron-electron correlation.
[46]J. C. Phillips, Phys. Rev. B **40**, 7348 (1989).
[47]H. L. Stormer, A. F. J. Levi, K. W. Baldwin, M. Anzlowar, and G. S. Boebinger, Phys. Rev. B **38**, 2472 (1988).
[48]M. Hawley *et al.*, Science **251**, 1587 (1991); C. Gerber *et al.*, Nature **350**, 2484 (1990).
[49]A. Inam *et al.*, Appl. Phys. Lett. **57**, 2484 (1990).
[50]T. F. Rosenbaum, S. People, R. N. Bhatt, and T. V. Ramakrishnan, Phys. Rev. B **42**, 12 214 (1990). The simplest way to understand the magnetic freeze-out reported by these authors is to note that, when $\hbar\omega_c > \Delta_{cc}$ (where Δ_{cc} is the central cell or valley-orbit splitting), the valley-orbit degrees of freedom normal to the field are frozen out. In Ge there are four such degrees of freedom-impurity, and thus the number of degrees of freedom is reduced to $4(d-1)/d=\frac{8}{3}$ per impurity. See J. C. Phillips, Solid State Commun. **47**, 191 (1983) for a concise topological summary of the general principles of localization.
[51]A. Nitzan, K. F. Freed, and M. H. Cohen, Phys. Rev. B **15**, 4476 (1977).
[52]J. H. van Vleck, *Electric and Magnetic Susceptibilities* (Oxford University Press, New York, 1932), p. 94.
[53]T. Penney, S. von Molnar, D. Kaiser, F. Holtzberg, and A. W. Kleinsasser, Phys. Rev. B **38**, 2918 (1988).
[54]T. R. Nichols *et al.*, Physica B **169**, 633 (1991).
[55]O. Laborde *et al.*, Phys. Lett. A **147**, 525 (1990).
[56]M. Affronte, M. Decroux, W. Sadowski, T. Graf, and O. Fischer, Physica C **172**, 131 (1990).
[57]J. C. Phillips, Phys. Rev. B **43**, 11 415 (1991).
[58]T. Penney, M. W. Shafer, B. L. Olsen, and T. S. Plaskett, Adv. Ceram. Mat. **2**, 577 (1987). Note that epitaxial films of $La_{2-x}Sr_xCuO_4$ exhibit the usual linear freeze-out and patch upturn temperature dependence, M. Suzuki and T. Murakami, Jpn. J. Appl. Phys. **26**, L524 (1987).
[59]S. K. Agarwall, R. Suryanarayanan, O. Gorochov, V. N. Moorthy, and A. V. Narlikar, Solid State Commun. **79**, 857 (1991).
[60]D. P. Norton *et al.*, Phys. Rev. Lett. **66**, 1537 (1991).
[61]P. M. J. Marée *et al.*, J. Appl. Phys. **62**, 4413 (1987).
[62]N. F. Mott, Philos. Mag. Lett. **62**, 273 (1990).
[63]F. Sharifi, A. Pargellis, and R. C. Dynes, Phys. Rev. Lett. **67**, 509 (1991).
[64]C. Homes *et al.*, Phys. Rev. Lett. **67**, 2694 (1991).
[65]J. C. Phillips (unpublished); K. M. Rabe, J. C. Phillips, and P. Villars, J. Non-Cryst. Solids (to be published).
[66]J. C. Phillips and K. M. Rabe, Phys. Rev. Lett. **66**, 923 (1991).
[67]U. Mizutani *et al.*, J. Phys. Condens. Matter **2**, 6169 (1990).
[68]J. C. Phillip, Solid State Commun. **47**, 191 (1983); Europhys. Lett. **14**, 367 (1991); Phys. Rev. B **41**, 8968 (1990); **42**, 2825

(1990); **45**, 5863 (1992).
[69]H. Spohn, J. Phys. A **19**, 533 (1986); B. Gerlach and H. Löwen, Rev. Mod. Phys. **63**, 63 (1991).
[70]C. Chaillout *et al.*, Physica C **181**, 325 (1991). Noncubic diffraction anomalies associated with Bi have also been found by H. D. Rosenfeld and T. Egami (unpublished) in superconductive $Ba_{0.6}K_{0.4}BiO_3$.
[71]H. Takagi *et al.*, Phys. Rev. Lett. **68**, 3777 (1992).
[72]T. R. Thurston *et al.*, Phys. Rev. B **39**, 4327 (1989).
[73]H. Fukuyama, Physica C **185**, xxv (1991).
[74]P. W. Anderson, Physica C **185**, 11 (1991).
[75]J. R. Schrieffer, Physica C **185**, 17 (1991).
[76]X.-D. Xiang *et al.*, Phys. Rev. Lett. **68**, 530 (1992).
[77]B. Horovitz, G. R. Barsch, and J. A. Krumhansl, Phys. Rev. B **36**, 8895 (1987).
[78]G. Cannelli *et al.*, Phys. Rev. B **45**, 931 (1992).
[79]J. C. Phillips, Phys. Rev. B **40**, 8774 (1989). Another argument is that strong coupling at defects is precluded by self-consistent screening, but this argument does not include local-field corrections. For complex systems there is no principle which forbids strong local electron-phonon coupling.
[80]P. E. A. Turchi, Phys. Rev. Lett. **67**, 1779 (1991).
[81]L. Reinhard, B. Schönfeld, G. Kostorz, and W. Bührer, Phys. Rev. B **41**, 1727 (1990).
[82]J. A. Rayne, Phys. Rev. **110**, 606 (1958).
[83]J. M. Ziman, Adv. Phys. **10**, 2 (1961).